Molecular Crystals and Liquid Crystals

Publication details, including instructions for authors and subscription information:
http://www.tandfonline.com/loi/gmcl20

Low Threshold DFB Lasing at the Edge and Defect Modes in Chiral Liquid Crystals

V. A. Belyakov [a]

[a] L. D. Landau Institute for Theoretical Physics, Moscow, Russia

Version of record first published: 22 Sep 2010

To cite this article: V. A. Belyakov (2008): Low Threshold DFB Lasing at the Edge and Defect Modes in Chiral Liquid Crystals, Molecular Crystals and Liquid Crystals, 488:1, 279-308

To link to this article: http://dx.doi.org/10.1080/15421400802241134

Mol. Cryst. Liq. Cryst., Vol. 488, pp. 279–308, 2008

ISSN: 1542-1406 print/1563-5287 online
DOI: 10.1080/15421400802241134

Taylor & Francis
Taylor & Francis Group

Low Threshold DFB Lasing at the Edge and Defect Modes in Chiral Liquid Crystals

V. A. Belyakov
L. D. Landau Institute for Theoretical Physics, Moscow, Russia

A brief survey of the recent experimental and theoretical results on the low threshold distributed feedback (DFB) lasing in chiral liquid crystals (CLC) as well as new original theoretical results in the field are presented. The presentation is concentrated on the lasing thresholds at frequencies corresponding to the stop band edge lasing modes and defect modes in CLC. It is demonstrated that the analytic approach reproduces all features of the DFB lasing in CLC obtained by the traditional numerical approach and, more over, allows to reveal some qualitative effects escaped from the researchers employing the numerical methods. Namely, the effect of anomalously strong absorption at the defect mode frequency, a direct analogue of the corresponding effect at the stop band edge mode frequency, is predicted in the framework of the analytic approach. It is proposed also to reduce the lasing threshold by adjusting the pumping wave to the conditions of the anomalously strong absorption effect at the defect mode frequency. The developed approach helps to clarify the physics of lasing at the stop band edge and defect modes in CLC and manifests an agreement with the corresponding results of the previous investigations obtained by a numerical approach.

Keywords: anomalous absorption; chiral LC; defect and stoop band edge modes; low threshold lasing

INTRODUCTION

Recently there was a very intense activity in the field of the stop band edge and defect electromagnetic modes in chiral liquid crystals mainly due to the possibilities to reach a low lasing threshold for the mirrorless distributed feedback (DFB) lasing [1–4], to use these modes as narrow band filters [5,6] and to enhance the nonlinear optical high harmonic generation [7] in chiral liquid crystals.

Address correspondence to V. A. Belyakov, L.D. Landau Institue for Theoretical Physics, Kosygin Str. 2, Mosocow 117334, Russia. E-mail: bel@landau.ac.ru

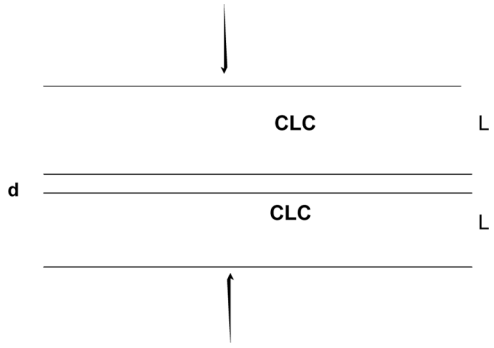

FIGURE 1 Schematic of the CLC defect mode structure with an isotropic defect layer.

The experiments showed that in a perfect chiral liquid crystal layer a low threshold lasing occurs at the frequencies close to the stop band edges [8–13]. For the lasing at defect mode structures (see Fig. 1) the lasing frequency is situated inside the stop band frequency range and the lasing threshold is lower than the corresponding threshold for lasing close to the stop band frequencies [1,2,3,14,15] (in the same experiment may be observed both the edge lasing frequency and the lasing at the frequencies inside the stop band).

In general, the theory of the DFB lasing in chiral liquid crystals is very similar to the theory of the DFB lasing in conventional solid periodic media which initially was developed by Kogelnik [16] in the coupled wave approximation and later was treated by the analogous way in many papers [17,18].

The edge and defect modes existing as a localized electromagnetic eigen state at stop band edge and within the forbidden band gap at the structure defect were theoretically investigated initially in the three-dimensionally periodic dielectric structures [5,16]. The corresponding modes in chiral liquid crystals, and more general in spiral media, are very similar to the defect modes in one-dimensional scalar periodic structures. They reveal abnormal reflection and transmission at the edge and inside the forbidden band gap [1,2] and allow DFB lasing at a low lasing threshold [3]. The qualitative difference with the case of scalar periodic media consists in the polarization properties. The edge and defect modes in chiral liquid crystals are associated with a circular polarization of the electromagnetic field eigen state of the chirality sense coinciding with the one of the chiral liquid crystal helix. There are two types of defects in chiral liquid crystals studied up to now. One of them is an isotropic plane layer of some thickness dividing

in two parts a perfect cholesteric structure and being perpendicular to the helical axes of the cholesteric structure [1]. Other one is a jump of the cholesteric helix phase at some plane perpendicular to the helical axes (without insertion any substance at the location of this plane) [2]. Recently, a new type of defect layer was studied [19], namely, the CLC layer with the pitch differing from the pitch of two layers sandwiching the defect layer. It is evident that there are many versions of the dielectric properties of the defect layer, however, the consideration below will be limited by the mentioned above two main types of defects in chiral liquid crystals.

Almost all theoretical studies of the edge and defect modes in chiral and scalar periodic media were performed by means of a numerical analysis with one exception [20], where the known exact analytical expression for the eigen modes propagating along the helix axes [21,22] were used for a general studying of the defect mode associated with a jump of the helix phase. The used in [20] approach looks as a very fruitful one because it allows to reach easy understanding of the defect mode physics and it is why it deserves further implementation in the studying of the edge and defect modes and, in particular, in specific cases allowing essential simplification of the general relationships related to the defect modes. In general, the helical media are the unique periodic structure admitting a simple exact analytic solution of Maxwell equations and, naturally, this advantage of the helical media compared to the other periodic media has to be completely exploited in solving specific boundary problems, related to the edge and defect modes. In the present paper an analytical solution of the defect mode associated with an insertion of an isotropic layer in the perfect cholesteric structure is presented and some limiting cases simplifying the problem are considered. The obtained results are directly applicable to chiral ferroelectric liquid crystals for the considered here case of light propagating along the spiral axes because for this case the optical properties of a cholesteric and a chiral ferroelectric liquid crystal are identical [23–25].

GENERAL EQUATIONS

To consider the defect mode associated with an insertion of an isotropic layer in the perfect cholesteric structure we have to solve Maxwell equations and a boundary problem for electromagnetic wave propagating along the cholesteric helix for the layered structure depicted at Figure 1. To find solutions corresponding to the edge modes one needs to solve the boundary problem only for one CLC layer depicted at Figure 1, i.e. for one half of Figure 1 [24,25].

The Maxwell equations for the wave propagating along the helix axes has the following form

$$\delta^2\mathbf{E}/\delta z^2 = \mathrm{c}^{-2}\boldsymbol{\varepsilon}(\mathrm{z})\delta^2\mathbf{E}/\delta^2\mathrm{t}, \tag{1}$$

where $\varepsilon(\mathrm{z})$ is the dielectric tensor of the cholestric liquid crystal [23–25] and z-axes is directed along the helix axes.

As it is well known in the perfect cholesteric structure, i.e. in each cholesteric layer depicted at Figure 1 there are four eigen solutions of Maxwell equations (first studied in [21,22]) each of them being a superposition of two plane wave. Two of these eigen solutions correspond to the wave nondiffracting in the cholesteric and two other correspond to the wave diffracting in the cholesteric and having one frequency band (around so called Bragg frequency) forbidden for propagation of the wave. The diffracting eigen solutions are related to the circular polarization with the same sense of chirality as the chirality sense of the cholesteric helix and the nondiffracting eigen solutions are related to the circular polarization with the opposite sense of chirality. So solving the boundary problem one has to present electromagnetic wave in the cholesteric as a linear superposition of the four eigen solutions in each cholesteric layer of the structure depicted at Figure 1 For a whole structure the boundary problem is reduced to the four problems related to the four interfaces of the structure. Except the parameters entering in the eigen solutions (see below) the mentioned system contains as a parameter, in particular, the ration of the dielectric constant of the defect layer to the average dielectric constant of the cholesteric. So, if one assumes a simple dielectric properties of the defect layer (its isotropy, for example) the exact solution of the boundary problem is presented analytically as a solution of the system of 8 linear equations. Zero value of the determinant of this system determines the eigen solution of the boundary problem, i.e. the defect mode. However, the corresponding analytical solution and the equation determining the eigen mode are sufficiently cumbersome in the general case.

In the result of a general analysis of the solution of the formulated boundary problem and the boundary problem for a single cholesteric layer [24,25] one concludes that no truly localized defect mode exists for the boundary problem under consideration. The reason for such conclusion is based on the fact that at the isotropic layer boundaries there is a conversion of the diffracting eigen solutions into the nondiffracting eigen solutions escaping out of the external cholesteric layer surfaces. However in the most favorable case when the dielectric constant of the defect layer is equal to the average dielectric constant of the cholesteric the conversion of polarization is low (proportional to

the dielectric anisotropy of the cholesteric) and one may say in the general case about quasi localized defect mode (see also [20] for the defect modes related to the helix phase jump).

To clarify the general results we shall present in the next sections the explicit form of the eigen solutions and the specific cases simplifying solution of the boundary problem, namely case of the dielectric constant of the isotropic defect layer being equal to the average dielectric constant of the cholesteric and, in particular, the case of diffractionally thick cholesteric layers at Figure 1.

EIGEN WAVES IN CHIRAL LC

As it is known [21–25] the eigenwaves corresponding to propagation of light in chiral LC along the spiral axis, i.e. the solution of the Maxwell equation (1) are presented by a superposition of two plane waves of the form

$$\mathbf{E}(z,t) = e^{-i\omega t}[E^{+}\mathbf{n}_{+}\exp(i\mathbf{K}^{+}\mathbf{z}) + E^{-}\mathbf{n}_{-}\exp(i\mathbf{K}^{-}\mathbf{z})] \tag{2}$$

where ω is the light frequency, $\mathbf{n}_{\pm}$ are the two vectors of circular polarizations, c is the light velocity and the wave vectors $\mathbf{K}^{\pm}$ satisfy to the condition

$$\mathbf{K}^{+} - \mathbf{K} = \tau, \tag{3}$$

where τ is the reciprocal lattice vector of the LC spiral ($\tau = 4\pi/p$, where p is the cholesteric pitch).

The wave vectors $\mathbf{K}^{\pm}$ in four eigen solutions of (1) are determined by the Eq. (3) and the following formulas

$$\mathbf{K}_{j}^{+} = \tau/2 \pm \kappa\{1 + (\tau/2\kappa)^2 \pm [(\tau/\kappa)^2 + \delta^2]^{\frac{1}{2}}\}^{\frac{1}{2}}, \tag{4}$$

where j numerates the eigen solutions with the ratio of amplitudes (E^{-}/E^{+}) in (2) given by the expression

$$\xi^{j} = (\mathbf{E}^{-}/\mathbf{E}^{+})_{j} = \delta/[(\mathbf{K}_{j}^{+} - \tau)^2/\kappa^2 - 1], \tag{5}$$

where $\kappa = \omega\varepsilon_0^{\frac{1}{2}}/c$, $\varepsilon_0 = (\varepsilon_{||} + \varepsilon_{\perp})/2$, $\delta = (\varepsilon_{||} - \varepsilon_{\perp})/(\varepsilon_{||} + \varepsilon_{\perp})$ is the dielectric anisotropy, and $\varepsilon_{||}$, $\varepsilon_{\perp}$ are the principal values of the LC dielectric tensor [21–25]. Two of the eigen waves corresponding to the circular polarization with the sense of chirality coinciding with the one of the LC spiral experience strong diffraction scattering at the frequencies in the region of the stop band. Other two eigenwaves corresponding to the opposite circular polarizations are almost not influenced by the diffraction scattering even at the frequencies of the stop band for the former circular polarization.

Because, as it is known [2,3,20], the specific of the defect modes in chiral LC is connected with the eigen waves of diffracting polarization we shall limit ourselves below by the consideration of propagation of light of a diffracting polarization only.

BOUNDARY PROBLEM

In this section the boundary problem discussed above in a general form will be considered under assumption that the specific parameters of the problem allow simplification of the mentioned equtions. We shall assume (see Fig. 1) that the chiral LC is presented by a planar layer with a spiral axes perpendicular to the layer surfaces. We shall also assume that the average dielectric constant of the CLC ε_0 coincides with the dielectric constant of the isotropic external medium and the isotropic layer inserted between two cholestric layers. This assumption allows to regard the conversion of one circular polarization to another one at the layer surfaces as negligible [24,25] because it is proportional to the small parameter δ, the cholesteric dielectric anisotropy, and allows one to take into account in the consideration only two eigen waves (and correspondingly only two wave vectors from Eq. (4)) with diffracting circular polarization.

Begin the consideration of a linear boundary problem in the formulation which assumes that two plane waves of the diffracting polarization and of the same frequency are incident along the spiral axis at the both CLC layers (see Fig. 1) from the opposite sides and the dielectric tensor may have non zero imaginary part of any sign. Two diffracting eigen solutions with the structure determined by Eq. (2) are exited in the both cholesteric layers. The amplitudes of the two diffracting eigenwaves denoted $\mathrm{E}_{+}^{+\mathrm{u}}$ and $\mathrm{E}_{-}^{+\mathrm{u}}$ for the upper and $\mathrm{E}_{+}^{+\mathrm{d}}$ and $\mathrm{E}_{-}^{+\mathrm{d}}$ for the bottom layer, respectively, have to satisfy to the following system of four linear equations [24,25] (as the results of continuity of the tangential components of the electric and magnetic fields at the 4 boundaries of cholesteric layers depicted at Fig. 1)

$$\mathrm{E}_{+}^{+\mathrm{u}} + \mathrm{E}_{-}^{+\mathrm{u}} = \mathrm{E}_{\mathrm{iu}}$$

$$\begin{aligned}
&\exp[\mathrm{i}\ \mathrm{kd}]\ \exp[\mathrm{i}\ \mathrm{K}_{+}^{+}\mathrm{L}_{-}]\ \mathrm{E}_{+}^{+\mathrm{u}} + \exp[\mathrm{i}\ \mathrm{kd}]\ \exp[\mathrm{i}\ \mathrm{K}_{-}^{+}\mathrm{L}_{-}]\ \mathrm{E}_{-}^{+\mathrm{u}} \\
&\quad = \exp[\mathrm{i}\ \mathrm{K}_{+}^{+}\mathrm{L}_{+}]\ \mathrm{E}_{+}^{+\mathrm{d}} + \exp[\mathrm{i}\ \mathrm{K}_{-}^{+}\mathrm{L}_{+}]\ \mathrm{E}_{-}^{+\mathrm{d}} \\
&\xi^{+}\exp[\mathrm{i}\ \mathrm{K}_{+}^{-}\mathrm{L}_{-}]\ \mathrm{E}_{+}^{+\mathrm{u}} + \xi^{-}\exp[\mathrm{i}\ \mathrm{K}_{-}^{-}\mathrm{L}_{-}]\ \mathrm{E}_{-}^{+\mathrm{u}} \\
&\quad = \exp[\mathrm{ikd}]\xi + \exp[\mathrm{i}\ \mathrm{K}_{+}^{-}\mathrm{L}_{+}]\ \mathrm{E}_{+}^{+\mathrm{d}} + \exp[\mathrm{ikd}]\xi^{-}\exp[\mathrm{i}\ \mathrm{K}_{-}^{-}\mathrm{L}_{+}]\ \mathrm{E}_{-}^{+\mathrm{d}} \\
&\qquad \times \exp[\mathrm{i}\ 2\mathrm{K}_{+}^{-}\mathrm{L}]\xi^{+}\mathrm{E}_{+}^{+\mathrm{d}} + \exp[\mathrm{i}2\mathrm{K}_{-}^{-}\mathrm{L}]\ \xi^{-}\mathrm{E}_{-}^{+\mathrm{d}} = \mathrm{E}_{\mathrm{id}}
\end{aligned} \tag{6}$$

where E_{iu} and E_{id} are the amplitudes of the waves of diffracting polarization incident at the cholesteric layers from the top and the bottom of the structure at Figure 1, respectively, 2L is the whole CLC structure thickness, d is the isotropic layer thickness and $L_{\pm} = L \pm d/2$ and

$$\begin{aligned} &K_{\pm}^{+} = \tau/2 \pm q, \quad K_{\pm}^{-} = K_{\pm}^{+} - \tau = -\tau/2 \pm q, \\ &\xi^{\pm} = E_{\pm}^{-}/E_{\pm}^{+} = \delta/[(K_{\pm}^{+} - \tau)^2/\kappa^2 - 1], \end{aligned} \tag{7}$$

where $q = \kappa\{1 + (\tau/2\kappa)^2 - [(\tau/\kappa)^2 + \delta^2]^{\frac{1}{2}}\}^{\frac{1}{2}}$.

If one assumes E_{iu} (E_{id}) is the only nonzero amplitudes the Eq. (6) describes the reflection and transmission of light incident at the structure (Fig. 1) from above (down).

Consider now in more details the solutions of the system (6) in some specific situations.

PERFECT CHOLESTERIC LAYER

The case of perfect cholesteric layer corresponds to the two limits in Eq. (6) and is considered here for completeness of the present study (the corresponding results may be found also in [24,25]). One options corresponds to $d = 0$ and the second one to $d = 0$ and the thickness on of the layer at Figure 1 also equal to zero. The first and the second options correspond to a perfect CLC layer of thickness 2L and L, respectively. The solutions of the system (6) in these limits result in the following expressions for the amplitude reflection R and transmission T coefficients of a CLC layer of thickness L:

$$\begin{aligned} R(L) &= \delta \sin qL/\{(q\tau/\kappa^2)\cos qL + i[(\tau/2\kappa)^2 + (q/\kappa)^2 - 1]\sin qL\} \\ T(L) &= \exp[i\tau L/2](q\tau/\kappa^2)/\{(q\tau/\kappa^2)\cos qL + i[(\tau/2\kappa)^2 + (q/\kappa)^2 - 1]\sin qL\}, \end{aligned} \tag{8}$$

where the phases of T and R in (8) correspond to the assumption that the coordinate $z = 0$ at the entrance surface and correspondently the director orientation at the entrance surface is determined via the expression for the dielectric tensor of the cholestric liquid crystal $\varepsilon(z)$ [23–25] at $z = 0$.

INFINITELY THICK CLC LAYERS

Let us study the system (6) in the simplest case for very thick cholesteric layers at Figure 1. In this case the amplitudes of the eigen waves exponentially growing toward the external surfaces of cholesteric layers have to be zero. Formally, we may put L to be infinitely large.

So, in the cholesteric layers nonzero amplitudes correspond only to the eigen waves propagating toward the isotropic layer. It means that in the system (6) the amplitudes E_-^{+u} and E_+^{+d} are equal to zero and the system reduces to the following two linear equations.

$$\begin{aligned} \exp[\mathrm{i}\ \mathrm{kd}]\exp[\mathrm{i}\ K_+^+ L_-]\ E_+^{+u} &= \exp[\mathrm{i}\ K_-^+ L_+]\ E_-^{+d} \\ \xi^+ \exp[\mathrm{i}\ K_+^- L_-]\ E_+^{+u} &= \exp[\mathrm{ikd}]\ \xi^- \exp[\mathrm{i}\ K_-^- L_+]\ E_-^{+d} \end{aligned} \tag{9}$$

The defect mode in this case is determined by a zero value of the determinant of the system (9) reduced to the following condition:

$$\begin{aligned} -(2/\delta)\mathrm{Exp}[\mathrm{i}(\mathrm{k}-\mathrm{q})\mathrm{d}]\{(\tau\mathrm{q}/\kappa^2\}\cos(\tau/2-\mathrm{k})\mathrm{d} + \mathrm{i}[(\tau/2\kappa)^2 \\ + (\mathrm{q}/\kappa)^2 - 1]\sin(\tau/2-\mathrm{k})\mathrm{d}\} = 0. \end{aligned} \tag{10}$$

For the light frequencies inside the selective reflection band the value of the determinant (10) becomes zero if the isotropic layer thickness d is connected with the light frequency by the following relation:

$$\begin{aligned} (\mathrm{d}/\mathrm{p})(1-\mathrm{k}/(\tau/2)) = (1/2\pi)\mathrm{arc\,tg}[2(\tau/2\kappa)\{[4(\tau/2\kappa)^2 + \delta^2]^{\frac{1}{2}} \\ - 1 - (\tau/2\kappa)^2\}^{\frac{1}{2}}/[2(\tau/2\kappa)^2 \\ - [4(\tau/2\kappa)^2 + \delta^2]^{\frac{1}{2}}]] \end{aligned} \tag{11}$$

It means that the defect mode exists for any frequency inside the selective reflection band, however the existence condition demands specific value of the isotropic layer thickness for each chosen frequency value.

REFLECTION AND TRANSMISSION FOR DM STRUCTURE

As was mentioned the system (6) determines the amplitude light transmission T(d,L) and reflection R(d,L) coefficients for the DM structure if one of the amplitudes E_{iu} or E_{id} is assumed to be zero.

For the finite value of L one has to solve the system (6). The determinant of the system (6) is given by the expression

$$\begin{aligned} \mathrm{Det}(\mathrm{d},\mathrm{L}) = 4\{\exp(2\mathrm{ikd})\sin^2\mathrm{qL} - \exp(-\mathrm{i}\tau\mathrm{L})[(\tau\mathrm{q}/\kappa^2)\mathrm{cosqL} \\ + \mathrm{i}((\tau/2\kappa)^2 + (\mathrm{q}/\kappa)^2 - 1)\mathrm{sinqL}]^2/\delta^2]. \end{aligned} \tag{12}$$

zero values of which determine the defect mode frequencies.

However there is another option to obtain formulas determining the optical properties of the structure depicted at Figure 1. If one uses the expressions for the amplitude transmission T(L) and reflection R(L) coefficient (8) for a single cholesteric layer [24,25] the transmission

$|T(d,L)|^2$ and reflection $|R(d,L)|^2$ intensity coefficients for the whole structure may be presented in the following form:

$$|T(d,L)|^2 = |[T_e T_d \exp(ikd)]/[1 - \exp(2ikd) R_d R_u]|^2, \quad (13)$$

$$|R(d,L)|^2 = |\{R_e + R_u T_e T_u \exp(2ikd)/[1 - \exp(2ikd) R_d R_u]\}|^2, \quad (14)$$

where $R_e(T_e)$, $R_u(T_u)$ and $R_d(T_d)$ are the amplitude reflection (transmission) coefficients of the CLC layer (8) (see Fig. 1) for the light incidence at the outer (top) layer surface, for the light incidence at the inner top CLC layer surface from the inserted defect layer and for the light incidence at the inner bottom CLC layer surface from the inserted defect layer, respectively. It is assumed in the deriving of Eqs. (13,14) that the external beam is incident at the structure (Fig. 1) from the above only.

The Eqs. (13,14), as well as Eq. (12), may be used also for the determination of the defect mode frequencies. Namely, the defect mode frequencies correspond to zero values of the denominators of Eqs. (13,14).

NONABSORBING LC

Examine in more details the formulas of the preceding section for nonabsorbing cholesreic layers. The calculated intensity reflection ($|R(d,L)|^2$) and transmission ($|T(d,L)|^2$) spectra inside the stop band for the structure sketched at Figure 1 are presented at Figures 2,3. The figures show maxima in $|T(d,L)|^2$ and minima in $|R(d,L)|^2$ at some frequencies inside the stop band at positions which depend on the defect layer thickness d. As it is known [1–3,20], the corresponding minima and maxima frequencies correspond to the defect mode frequencies. For the layer thickness $d/p = 1/4$, what is just one half of the dielectric tensor period in a cholesteric, these maxima and minima are situated just at the stop band center. In the d/p interval $0 < d/p < 0.5$ the defect mode frequency value moves from the high frequency stop band edge to the low frequency stop band edge. At the further increase of the defect layer thickness the defect mode frequency oscillates between the high frequency and low frequency stop band edge. However it is trough if only Δkd is less than approximately 2π where Δk is the change of the wave vector at the frequency width of the stop band. When Δkd exceeds 2π the second defect mode frequency appears in the the stop band. Additional defect mode frequencies appear for a further growth of d and their number may be estimated as $\Delta kd/2\pi$. The described appearance of many defect mode frequencies inside the stop band is illustrated by Figures 4a,b. At Figure 4 only

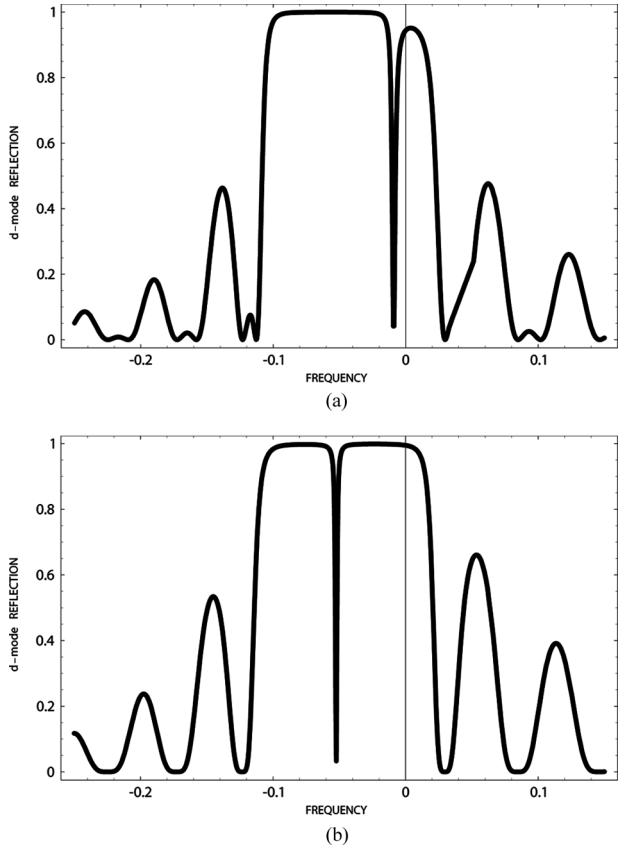

FIGURE 2 R(d) versus the frequency $(\nu = 2(\omega - \omega_B)/(\omega_B) - \delta)$ for a nonabsorbing CLC $(\gamma = 0)$ at $d/p = 0.1$ (a) and $d/p = 0.25$ (b); $\delta = 0.05$, $l = 200$, $l = L\tau = 2\pi N$, where N is the director half-turn number at the CLC layer thickness L.

$|T(d, L)|^2$ or $|R(d, L)|^2 = 1$ are presented because for a nonabsorbing structure $|T(d, L)|^2 + |R(d, L)|^2 = 1$.

The determined by Eq. (11) connection of the defect mode frequency with the isotropic layer thickness d for infinitely thick CLC layers is shown at Figure 5. Again the defect mode frequency (at Fig. 5) just at the stop band center corresponds to the layer thickness $d/p = 1/4$. The same results follows directly from (11) if one assumes $\tau/2\kappa = 1$:

$$d/p = (1/2\pi)\text{arc tg}[2/\{[4 + \delta^2]^{\frac{1}{2}} - 2\}^{\frac{1}{2}}] \approx (1/2\pi)\text{arc tg}[4/\delta] \qquad (15)$$

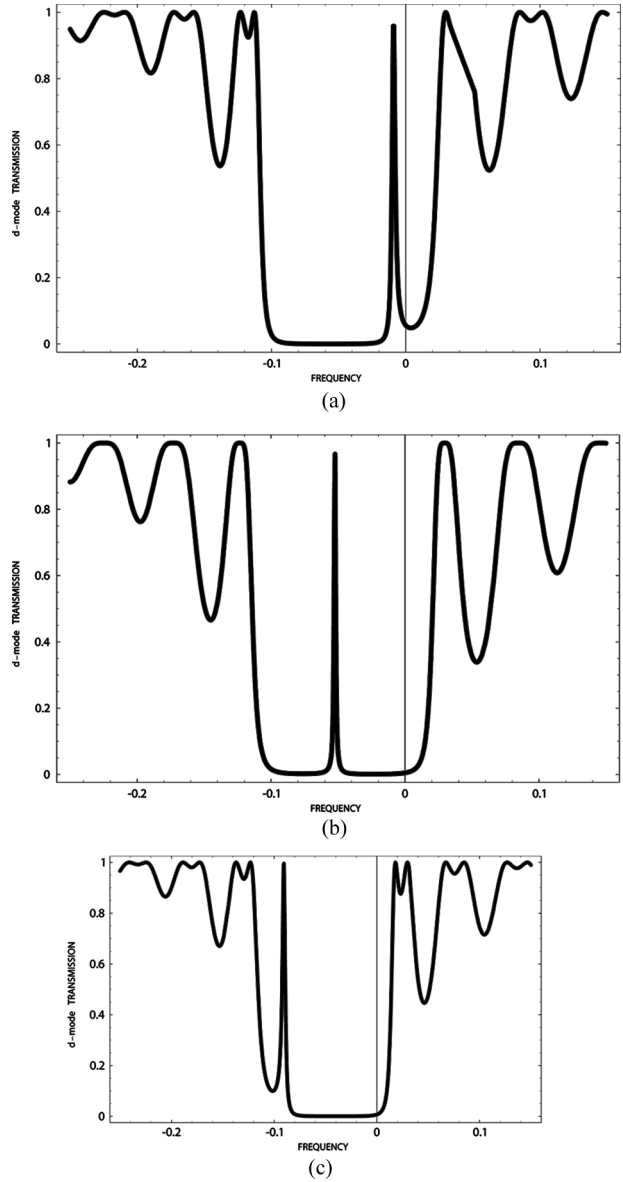

FIGURE 3 T(d) versus the frequency $(\nu = 2(\omega - \omega_B)/(\omega_B) - \delta)$ for a nonabsorbing CLC $(\gamma = 0)$ at $d/p = 0.1$ (a), $d/p = 0.25$ (b) and $d/p = 0.4$ (c); $\delta = 0.05$, $l = 200$, $l = L\tau = 2\pi N$, where N is the director half-turn number at the CLC layer thickness L.

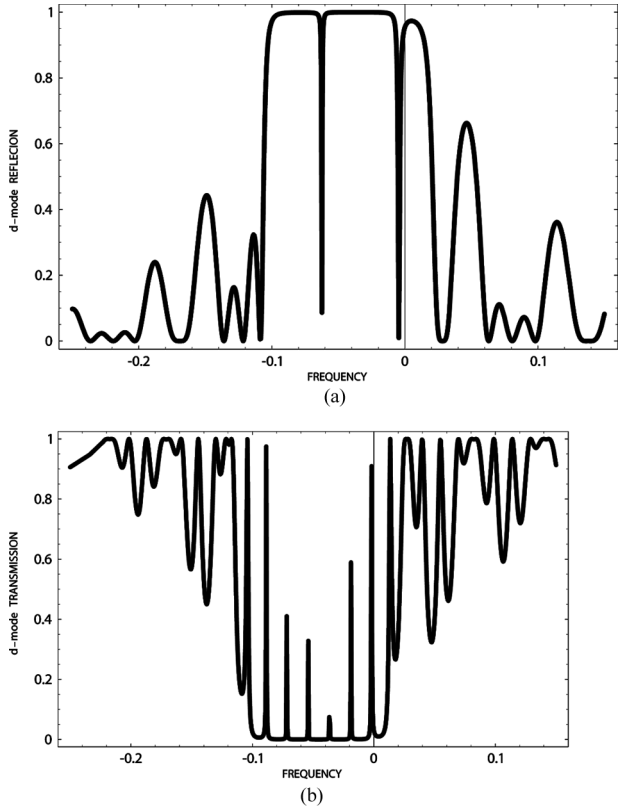

FIGURE 4 R(d) versus the frequency $(\nu = 2(\omega - \omega_B)/(\omega_B) - \delta)$ for a nonabsorbing CLC at d/p = 200.1 (a) and T(d) versus the frequency at d/p = 1000.6 1000.6 (b); $\delta = 0.05$, N = 33.

what corresponds approximately to d/p = 1/4 + n/2, where n is zero or an integer number.

The shift of the defect mode frequency $\Delta\omega$ in the interval $|\Delta\omega/\omega_B| < \delta$ due to a small variations of d (Δd) close to the d/p = 1/4 is given approximately by the relation

$$\Delta\omega/\omega_b = -4\Delta d/p, \tag{16}$$

where the Bragg frequency ω_B (frequency at the stop band centre) is $2\pi c/p\bar{\varepsilon}_0^{\frac{1}{2}}$.

As the calculations show the defect mode frequency is only slightly dependent on the CLC layer thickness L. It is why the found corresponding dependence for an infinitely large L may be regarded as a good approximation for any L.

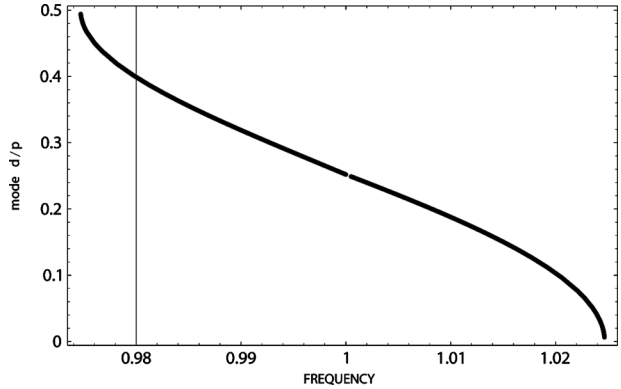

FIGURE 5 Calculated connection between d/p and the defect mode frequency ($v = \omega/\omega_B$) for nonabsorbing CLC layers of infinitely large thickness ($\delta = 0.05$).

The defect mode field is localized in the defect layer and close around it [1–3,16]. An illustration of the such localization is presented by the coordinate field distribution of a defect mode for infinitely thick CLC layers at Figure 6. The maximum of the field amplitude is located at the defect layer and the field amplitude attenuates exponentially in CLC outside of the defect layer. The most strong attenuation occurs for

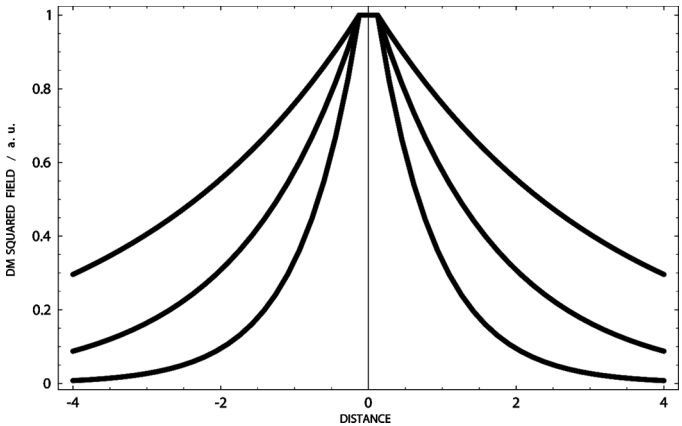

FIGURE 6 Calculated distribution of the squared field modulus versus the distance from the defect layer centre ($x = z/p$) for nonabsorbing infinitely thick CLC layers ($\delta = 0.05, 0.1, 0.2$ from the top curve to the bottom, respectively); $d/p = 1/4$.

the layer thickness d/p = 1/4, i.e. for the defect mode frequency just at the stop band centre, with decreasing of the attenuation upon approaching the defect mode frequency to the stop band edges. The attenuation growths also with the increase of the CLC layers dielectric anisotropy δ.

For infinitely thick CLC layers in the model under consideration the defect mode frequency is a real quantity and the defect mode life time is infinite. It is not the case for a limited CLC layer thickness. For

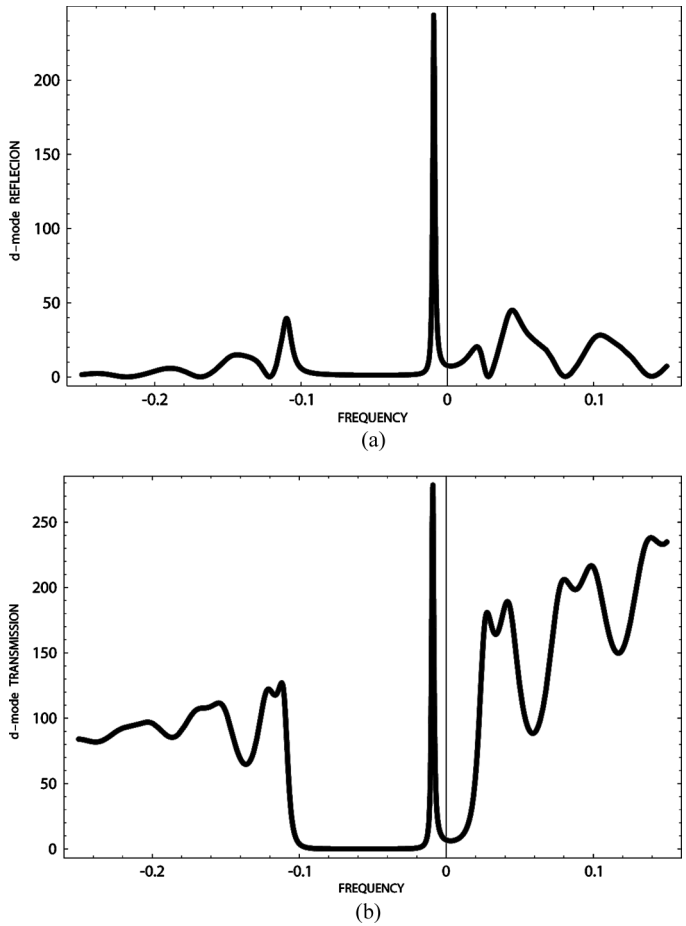

FIGURE 7 R(d) (a) and T(d) (b) versus the frequency $(\nu = 2(\omega - \omega_B)/(\omega_B) - \delta)$ for a nonabsorbing CLC at the complex addition to the frequency $(\omega/\mathrm{Re}[\omega] = (1 + \mathrm{is}))$ for s = -0.012 ; d/p = 0.1, $\delta = 0.05$, N = 33.

nonabsorbing CLC layers of finite thicknesses the determinant (12) reaches zero value for a complex frequency. The physical sense of a complex frequency is quite clear. For nonabsorbing CLC layers of a finite thickness there is a leakage of the defect mode electromagnetic field through the external surfaces of the CLC layers and, consequently, it results in a decay of the defect mode. Just the imaginary part of the frequency and the finite life time of the defect mode are determined by this leakage.

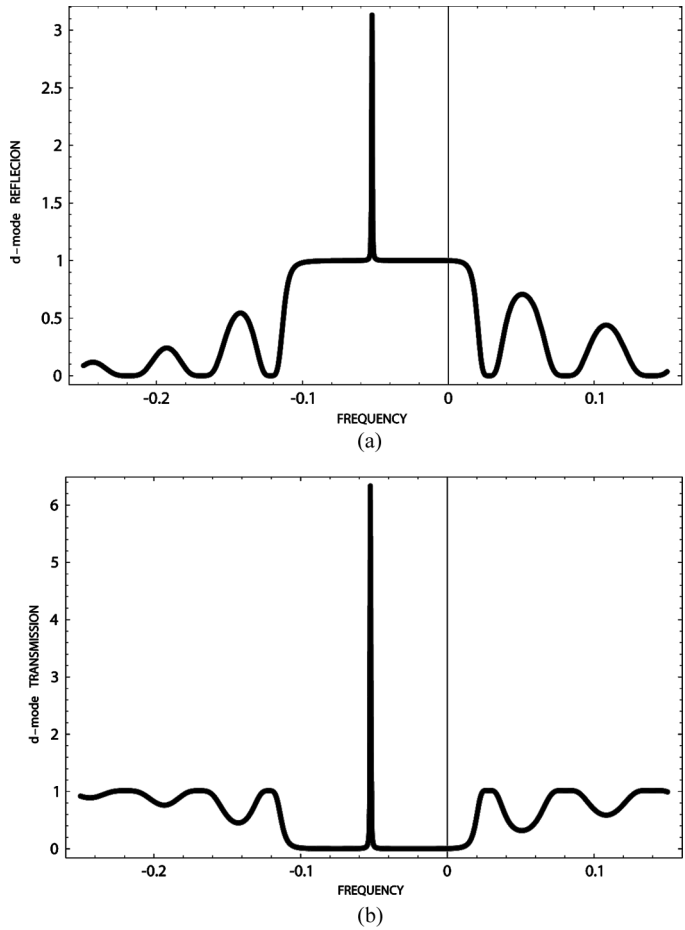

FIGURE 8 R(d) (a) and T(d) (b) versus the frequency $(\nu = 2(\omega - \omega_B)/(\omega_B) - \delta)$ for a nonabsorbing CLC at the complex addition to the frequency $(\omega/\mathrm{Re}[\omega] = (1 + \mathrm{is}))$ for $\mathrm{s} = -0.00466$; $\mathrm{d/p} = 1/4$, $\delta = 0.05$, $\mathrm{N} = 33$.

Instead of a direct solution of the equation for complex frequency following from the expression (12) (Det(d,L) = 0) the Eqs. (13,14) may be used also for the estimation of the imaginary part of defect mode frequency. One has to admit a non zero imaginary addition to the frequency (defined, for example, by the relation $\omega/\mathrm{Re}[\omega] = (1 + \mathrm{is})$, where s is a small quantity) and search for extremes of the Eqs. (13,14) relative to this imaginary addition. The corresponding calculations are presented at Figures 7,8. The calculations demonstrate that the imaginary addition decreases with the CLC layer thickness increase and the addition decreases also with approaching of the defect mode frequency to the stop band centre at fixed CLC layers thickness. The defect mode life time τ determined as $\tau = 1/|\mathrm{Im}\,\omega|$ grows correspondingly with the CLC layer thickness increase and reaches a maximum for the defect mode frequency at the stop band centre at fixed CLC layers thickness. The origin of a finite lifetime of the defect mode, i.e. leakage of the radiation from CLC layers of finite thickness, is illustrated by Figures. 9,10 where distribution of the field intensity versus the coordinate in the defect mode structure of finite thickness is given as well the distribution of the intensity of the field propagating toward the middle and out of the defect mode structure versus the coordinate are given. It happens that the energy flow outward of the defect mode structure of finite thickness always exceeds the energy flow inward the defect mode structure. It just means a decay of the defect mode.

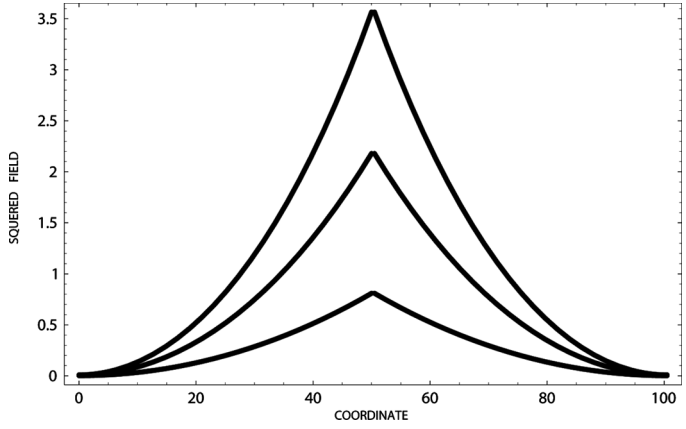

FIGURE 9 Coordinate dependence (in z/(p/2)) of the squared amplitude of the DM field (arbitrary units) at the DM frequency being at the stop band centre for various dielectric anisotropy values (from the top to the bottom $\delta = 0.05, 0.04, 0.025$) and the defect layer thickness d = p/4 for the cholesteric layer thickness L = 50 (p/2).

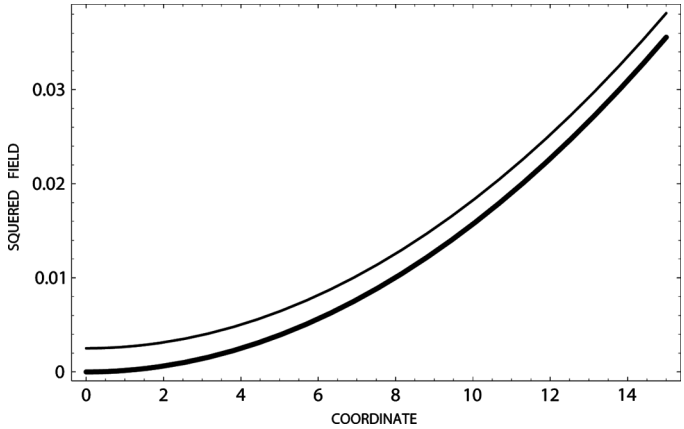

FIGURE 10 Coordinate dependence of the squared amplitude of the DM waves (arbitrary units) inside the CLC layer directed toward the defect layer (bold line) and out of the DM structure (narrow line) at the DM frequency being at the stop band centre for the dielectric anisotropy $\delta = 0.05$ close to the external surface of the CLC layer (z = 0 corresponds to the upper surface of the defect mode structure (Fig. 1)).

ABSORBING LC

Examine now the formulas (13,14) for absorbing cholesreic layers. For taking into account the absorption define the ratio of the dielectric constant imaginary part to the real part of ε as γ, i.e. $\varepsilon = \varepsilon_0(1 + i\gamma)$. Note, that in real situations $\gamma \ll 1$. A natural consequence of the non zero absorption, i.e. $\gamma > 0$, is reduction of the transmission $|\mathrm{T(d,L)}|^2$ and reflection $|\mathrm{R(d,L)}|^2$ coefficients. However there are some interesting peculiarities of the optical properties of the structure under consideration (Fig. 1). The calculation results presented at Figures 11–14 reveal these peculiarities. For absorbing structures $|\mathrm{T(d,L)}|^2 + |\mathrm{R(d,L)}|^2 < 1$ and the presented at Figures. 11–14 quantity $1 - |\mathrm{T(d,L)}|^2 + |\mathrm{R(d,L)}|^2$ gives a total absorption in the structure. Up to the relatively strong absorption ($\gamma = 0.005$ at Fig. 11) the spectral shapes of reflection and transmission conserve typical for the defect mode minima and maxima in reflection and transmission coefficients, respectively, nevertheless deviating from the case of nonabsorbing CLC (see Figs. 2,3). However, at the decrease of γ to a small value the spectral shapes of reflection and transmission are almost approaching to the case of nonabsorbing CLC (see Figs. 14 a,b corresponding $\gamma = 0.0003$).

What is concerned of the total absorption it demonstrates quite unusual frequency dependence. At a small γ for some frequencies

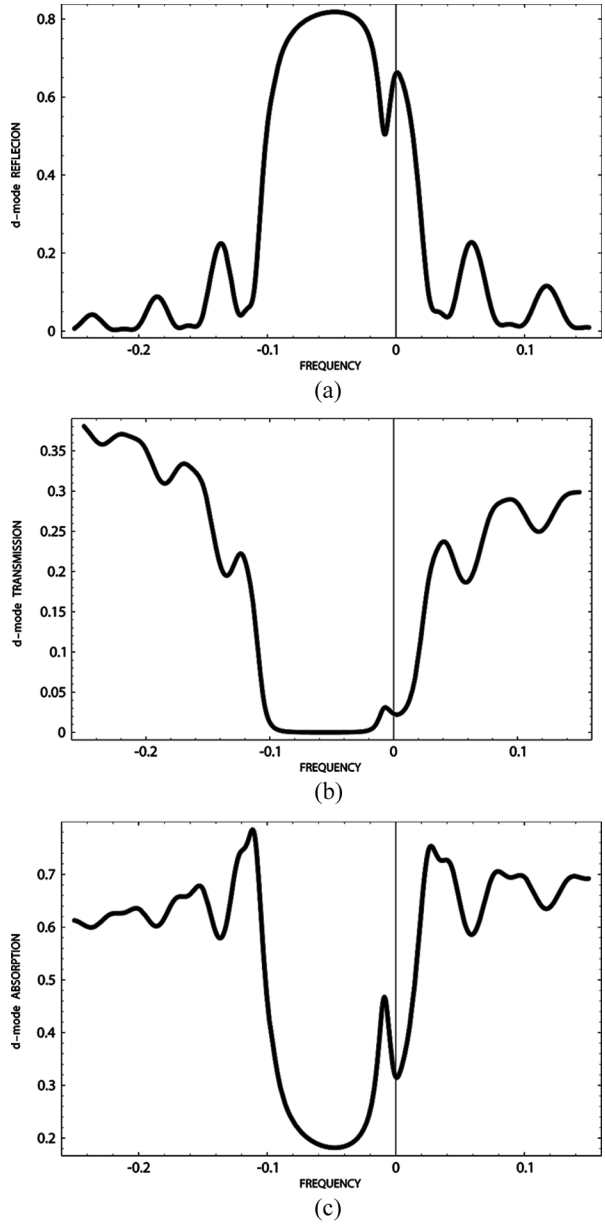

FIGURE 11 R(d) (a), T(d) (b) and the total absorption (c) for an absorbing CLC versus the frequency $(\nu = 2(\omega - \omega_B)/(\omega_B) - \delta)$, $\gamma = 0.005$; d/p = 0.1, $\delta = 0.05$, N = 33.

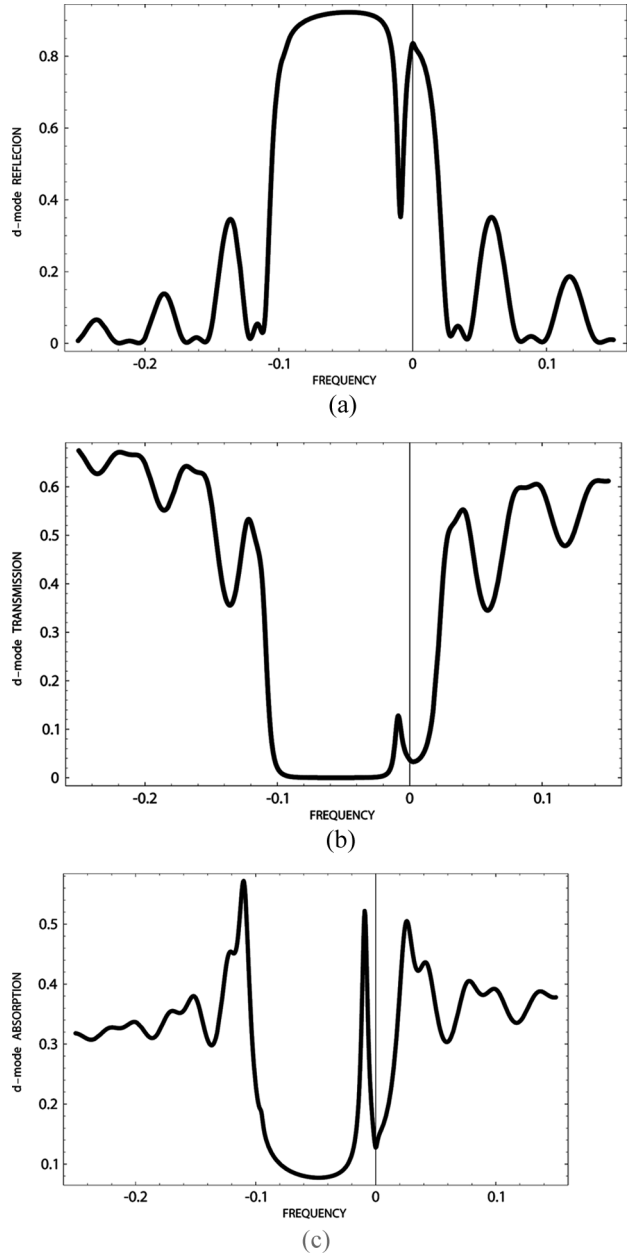

FIGURE 12 R(d) (a), T(d) (b) and the total absorption (c) for an absorbing CLC versus the frequency $(\nu = 2(\omega - \omega_B)/(\omega_B) - \delta)$, $\gamma = 0.002$; $d/p = 0.1$, $\delta = 0.05$, $N = 33$.

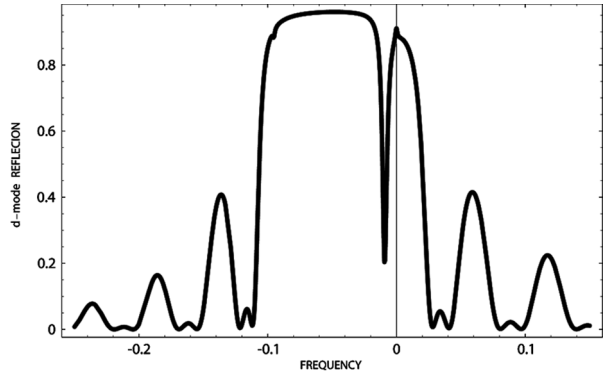

(a)

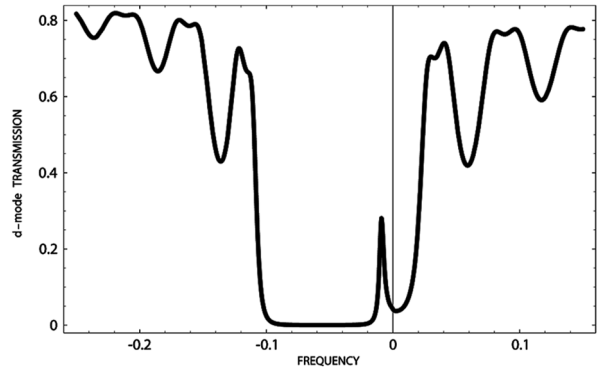

(b)

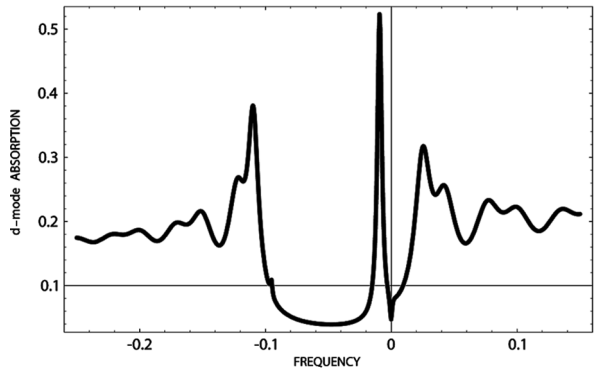

(c)

FIGURE 13 R(d) (a), T(d) (b) and the total absorption (c) for an absorbing CLC versus the frequency $(\nu = 2(\omega - \omega_B)/(\omega_B) - \delta)$, $\gamma = 0.001$; d/p = 0.1, $\delta = 0.05$, N = 33.

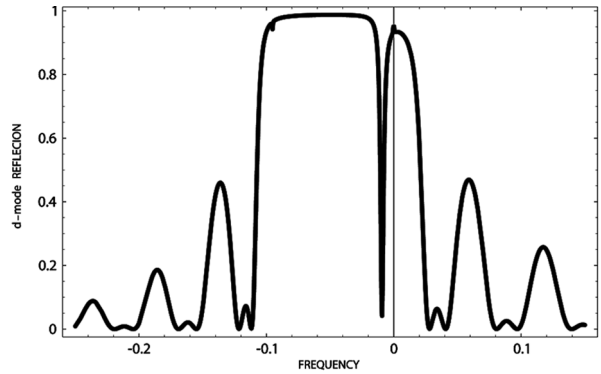

(a)

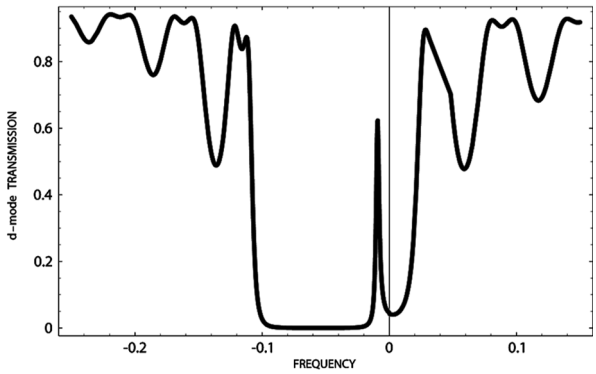

(b)

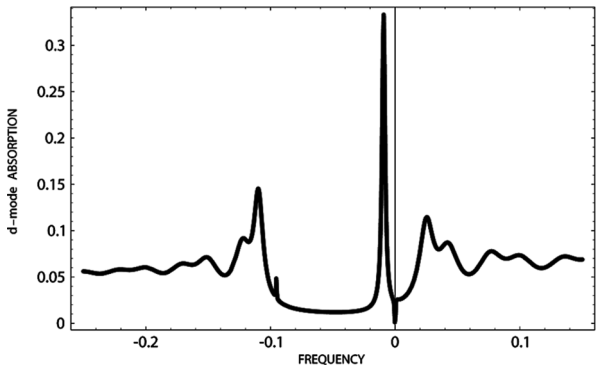

(c)

FIGURE 14 R(d) (a), T(d) (b) and the total absorption (c) for an absorbing CLC versus the frequency $(\nu = 2(\omega - \omega_B)/(\omega_B) - \delta)$, $\gamma = 0.0003$; d/p = 0.1, $\delta = 0.05$, N = 33.

the absorption occurs to be much more than the absorption out of the stop band (see Figs. 11–14). If γ is not too small (Fig. 11c, $\gamma = 0.005$) the total absorption increase reveals itself at the stop band edges (at the frequencies of the stop band edge modes). It is a manifestation of the so called "anomalously strong absorption effect" known for perfect CLC layers [25,26]. For a smaller γ the total absorption begins to exceed the absorption out of the stop band at the defect mode frequency being of the same value as for the stop band edge modes (Fig. 14c, $\gamma = 0.002$). At the further decrease of γ the anomalously strong absorption effect becomes more pronounced at the defect mode frequency than at the edge mode frequencies (Fig. 13c, $\gamma = 0.001$; Figure 14c, $\gamma = 0.0003$). As is clear, the anomalously strong absorption effect at the defect mode frequency is solely due to the localized defect mode, i.e. to the defect layer in the structure. Note, that the "anomalously strong absorption effect" at the defect mode frequency and its realization at some interrelation between γ and other LC parameters reveal themselves in the calculations of the total absorption at the defect mode frequency as a function of γ performed in [20] (the absorption reaches a maximum at a small finite value of γ, see Fig. 8 in [20]).

AMPLIFYING LC

Examine the formulas (13,14) for amplifying cholesreic layers. As above, we assume that the dielectric constant is presented by the same formula $\varepsilon = \varepsilon_0(1 + i\gamma)$, however with $\gamma < 0$. The calculation results for the intensity transmission $|T(d, L)|^2$ and reflection $|R(d, L)|^2$ coefficients at $\gamma < 0$ are presented at Figures 15–18. For a small absolute value of γ the shape of the transmission $|T(d, L)|^2$ and reflection $|R(d, L)|^2$ coefficients is qualitatively the same as for zero amplification ($\gamma = 0$) (Figs. 15a,b). The absorption, however, is a small negative quantity (what means amplification) at all frequencies with some amplification enhancement at the defect mode frequency and at the edge mode frequencies (Fig. 15c). For a growing absolute value of γ the shape of the reflection coefficient $|R(d, L)|^2$ changes at some value of γ (typical minimum in $|R(d, L)|^2$ is changed by a small maximum close to 1 and the transmission $|T(d, L)|^2$ exceeds 1 noticeably (Fig. 16)). At further increase of the absolute value of γ the reflection and transmission coefficients at the defect mode frequency for the chosen values of the problem parameters exceed one hundred (Fig. 17) with no signs of noticeable maxima at other frequencies. The corresponding value of γ may be considered as a close to the threshold value of the gain (γ) for the DFB lasing at the defect mode frequency. Continuing the increase of the absolute value of γ one finds that diverging

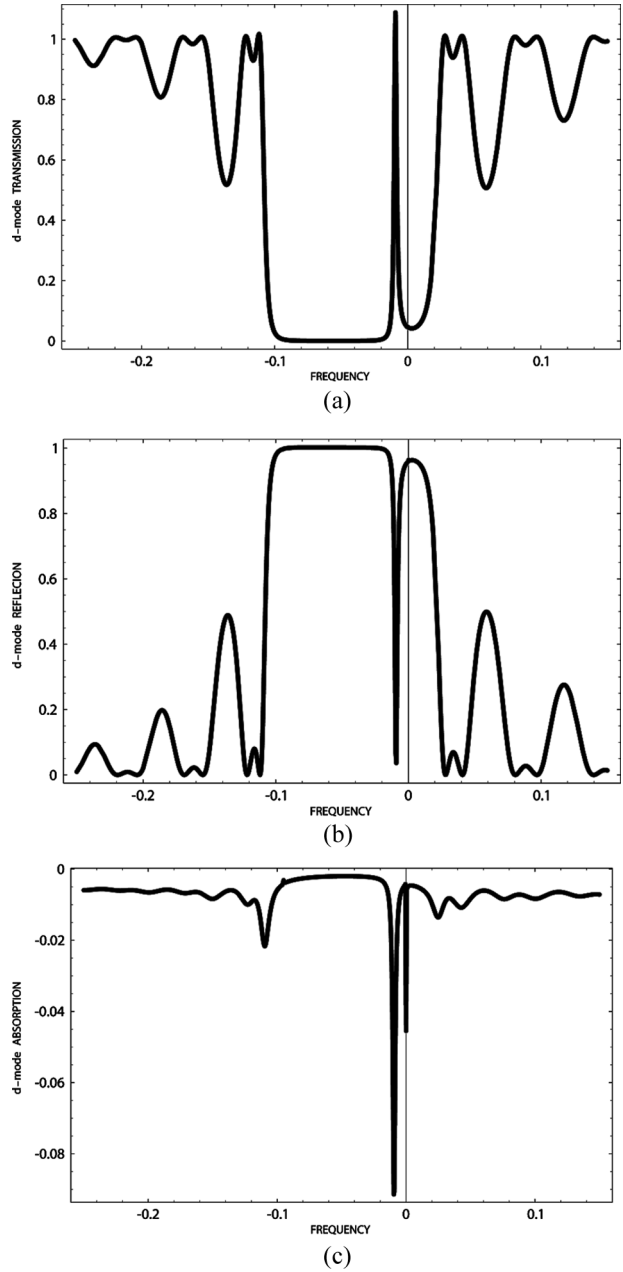

FIGURE 15 T(d) (a) and R(d) (b) for an amplifying CLC versus the frequency $(\nu = 2(\omega - \omega_B)/(\omega_B) - \delta)$, $\gamma = -0.00005$; $d/p = 0.1$, $\delta = 0.05$, $N = 33$.

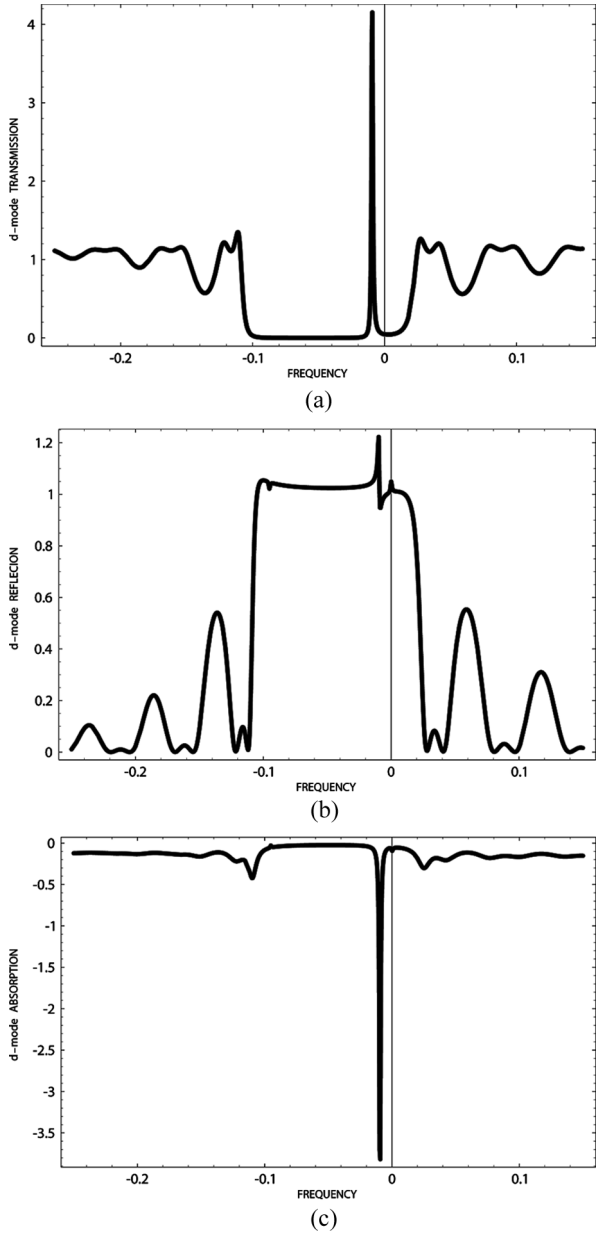

FIGURE 16 T(d) (a), R(d) (b) and the total absorption (c) for an amplifying CLC versus the frequency ($\nu = 2(\omega - \omega_B)/(\omega_B) - \delta$), $\gamma = -0.0006$; d/p = 0.1, $\delta = 0.05$, N = 33.

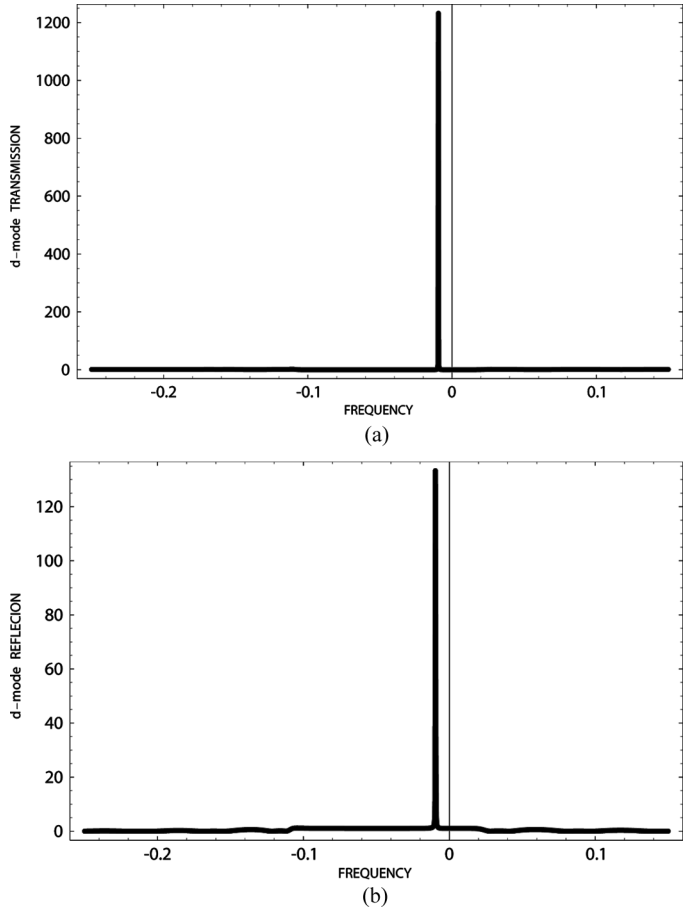

FIGURE 17 T(d) (a) and R(d) (b) for an amplifying CLC versus the frequency ($\nu = 2(\omega - \omega_B)/(\omega_B) - \delta$), $\gamma = -0.00117$; d/p = 0.1, $\delta = 0.05$, N = 33.

maxima at the edge mode frequencies appear (without no traces of maximum at the defect mode frequency) for the gain being five time more than the threshold gain for the defect mode (Fig. 18). At further continuing of the increase of the absolute value of γ one finds that in the lasing new edge mode frequencies, more distant from the stop band edge [27], appear. The observed result show that the defect mode lasing threshold gain is lower than the corresponding threshold for the stop band edge modes. Another conclusion following from this study is the revealed existence of some interconnection between the LC parameters at the lasing threshold which was found analytically for the edge modes

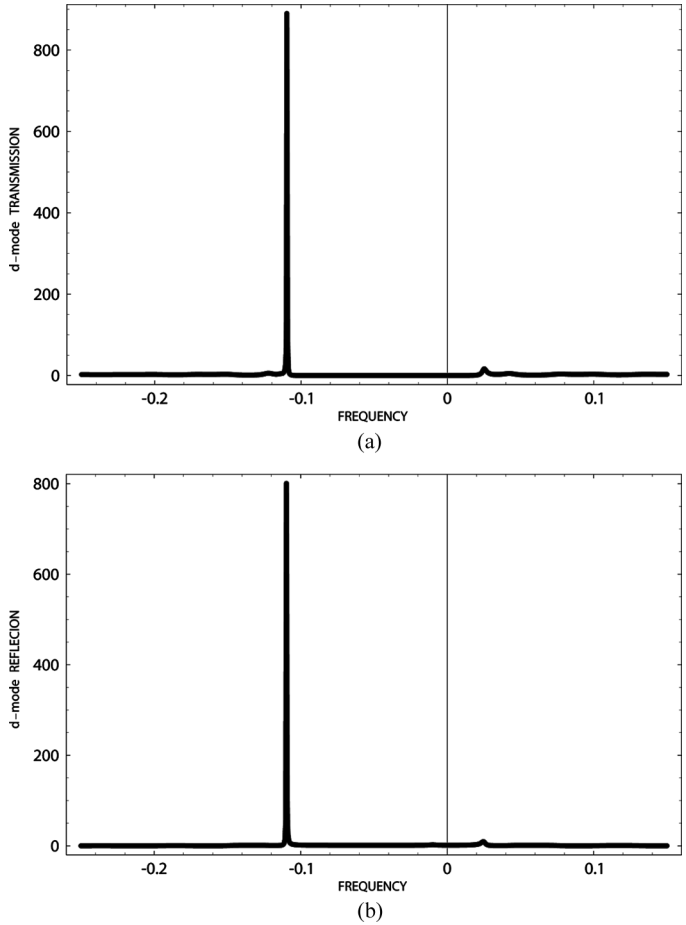

FIGURE 18 T(d) (a) and R(d) (b) for an amplifying CLC versus the frequency ($\nu = 2(\omega - \omega_B)/(\omega_B) - \delta$), $\gamma = -0.0045$; d/p = 0.1, $\delta = 0.05$, N = 33.

in [27]. Really, a continuous increase of the gain results in consequential appearance of a lasing at new modes with disappearance of lasing at the previous ones corresponding to more low thresholds.

At the Figure 19 the calculated different threshold values of γ corresponding to the different edge lasing modes for perfect LCL layers (divergent R and T at Figs. 19a–d) are presented. The Figure 19 shows that one is able to excite separate edge lasing modes by changing the gain (γ). If the value of γ is between the consequent threshold values of γ for neighboring lasing modes the lasing may not be achieved and the

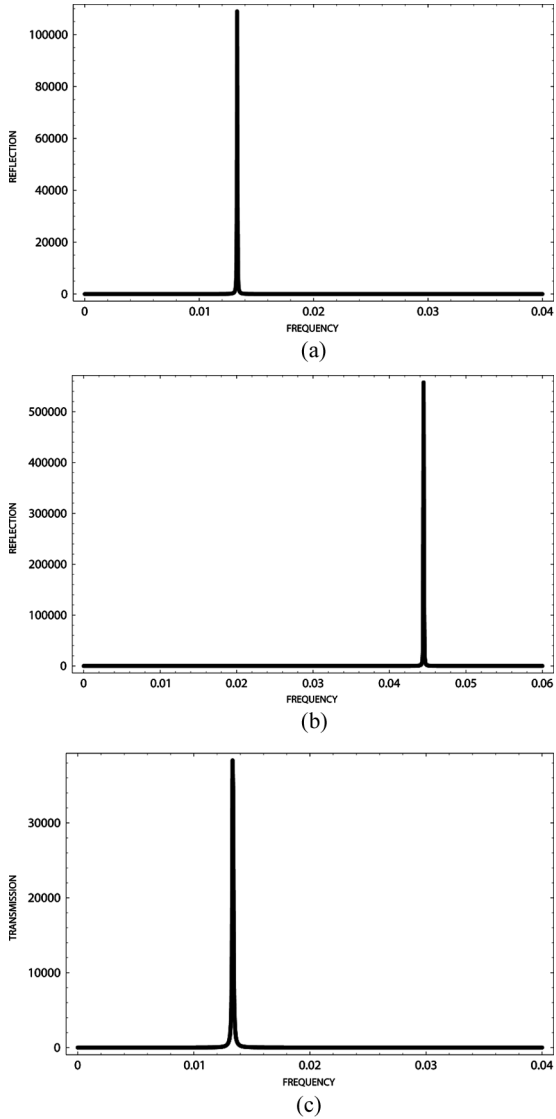

FIGURE 19 Calculated R versus the frequency ($\nu = 2(\omega - \omega_B)/\omega_B - \delta$, $\delta = 0.05$, $l = 300$, $l = L\tau$) (a) close to the threshold gain for the first lasing edge mode ($\gamma = -0.00565$), (b) close to the threshold gain for the second lasing edge mode ($\gamma = -0.0129$); calculated T versus the frequency ($\nu = 2(\omega - \omega_B)/\delta\omega_B - 1$, $l = 300$, $l = L\tau$) (c) close to the threshold gain for the first lasing edge mode ($\gamma = -0.00565$), (d) close to the threshold gain for the second lasing edge mode ($\gamma = -0.0129$).

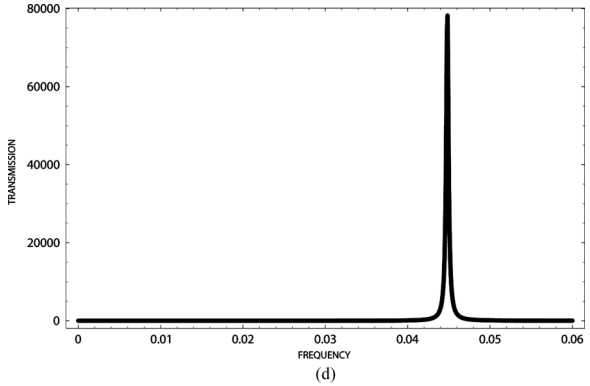

(d)

FIGURE 19 Continued.

layer may reveal only amplifying properties [27]. This means that changing of the pumping wave intensity allows to achieve lasing at the individual lasing modes and the lasing intensity is not monotonic function of the pumping intensity. Because the lasing frequency is determined by the edge lasing mode frequencies there is an option for some variation of the lasing frequency inside the width of the dye line by changing the CLC pitch by means of the temperature variations [11,12] or by application to the layer of external electric or magnetic field [10].

CONCLUSION

The performed above an analytic description of the defect modes neglecting the polarization mixing at the boundaries of CLC in the structure under consideration allows one to reveal clear physical picture of these modes which is applicable to the defect modes in general. For example, more low lasing threshold and more strong absorption (under the conditions of anomalously strong absorption effect) at the defect mode frequency compared to the edge mode frequencies are the features of any periodic media. Note, that the experimental studies of the lasing threshold [3] agree with the corresponding theoretical result obtained above. Moreover, the experiment [3] confirms also the existence of some interconnection between the gain and other LC parameters at the threshold pumping energy for lasing at the defect (as well at the stop band edge) mode frequency. Namely, an increase of the pumping energy above the threshold value results in decrease of the lasing intensity (see Fig. 5 in [3]).

For a special choice of the parameters in the experiment the obtained formulas may be directly applied to the experiment. However, in the general case one has take into account a mutual transformation at the boundaries of the two circular polarizations of opposite sense. For example, the observed in the experiment [3] circular polarization sense of the emitted from the defect structure wave above the lasing threshold may be opposite to the sense of the CLC spiral. An evident explanation of the "lasing" at the opposite (nondiffracting) circular polarization is in the following. Due to the polarization conversion a nondiffracting polarization freely escapes from the structure. This polarization conversion phenomenon adds also a contribution to the frequency width of the defect mode. So there is also need to take into account the polarization mixing in calculations of the defect mode life time (frequency width). In the general case the defect mode field leakage from the structure is determined as well by the finite CLC layer thickness so by the leakage due to the polarization conversion. Only for sufficiently thin CLC layers or in the case of the defect mode frequency being very close to the stop band frequency edges the main contribution to the frequency width of the defect mode is due to the thickness effect and the developed above model may be directly applied for describing of the experimental data.

It should be noted that the applied analytical approach facilitated to reveal the "anomalously strong absorption effect" at the defect mode frequency. The corresponding observation would be much more difficult to do at a purely numerical approach. Note,that the lowering of the lasing threshold due to the "anomalously strong absorption effect" at the edge mode frequency was observed recently for the collinear [28] and noncollinear [29] geometry of lasing

The defect type considered above is a homogenous layer. The developed approach is applicable also to a defect of "phase jump" type [2,3,20]. Taking into account the present results one may say in advance that, unlike for the considered homogenous layer defect, for a "phase jump" defect only one defect mode frequency inside the stop band frequency range is possible.

REFERENCES

[1] Yang, Y.-C., Kee, C.-S., & Kim, J.-E. et al. (1999). *Phys. Rev. E*, *60*, 6852.
[2] Kopp, V. I., & Genack, A. Z. (2003). *Phys. Rev. Lett.*, *89*, 033901.
[3] Schmidtke, J., Stille, W., & Finkelmann, H. (2003). *Phys. Rev Lett.*, *90*, 083902.
[4] Shibaev, P. V., Kopp, V. I., & Genack, A. Z. (2003). *J. Phys. Chem.*, *B 107*, 6961.
[5] Yablonovi tch, E., Gmitter, T. J., Meade, R. D. et al. (1991). *Phys. Rev. Lett.*, *67*, 3380.
[6] Hodgkinson, I. J., Wu, Q. H., Torn, K. E. et al. (2003). *Opt. Commun.*, *184*, 57.

[7] Hoshi, H., Ishikava, K., & Takezoe, H. (2003). *Phys. Rev. E*, *68*, 020701(R).
[8] Il'chishin, I. P., Tikhonov, E. A., Tishchenko, V. G., & Shpak, M. T. (1980). *JETP Lett.*, *32*, 24.
[9] Taheri, B., Muñoz, A. F., Palffy-Muhoray, P., & Twieg, R. (2001). *Mol. Cryst. Liq. Cryst. 358*, 73.
[10] Ozaki, M., Kasano, M., Kitasho, T., Ganzke, D., Haase, W., & Yoshino, K. (2003). *Adv. Mater.*, *15*(12), 974.
[11] Morris, S. M., Ford, A. D., Pivnenko, M. N., & Coles, H. J. (2005). *Journal of Applied Physics*, *97*(2), 023103.
[12] Chanishvili, A., Chilaya, G., Petriashvili, G., Barberi, R., Bartolino, R., Cipparrone, G., Mazzulla, A., Gimenez, R., Oriol, L., & Pinol, M. (2005). *Applied Physics Letters*, *86*, 055107.
[13] Finkelmann, H., Kim, S. T., Muñoz, A., Palffy-Muhoray, P., & Taheri, B. (2001). *Adv. Mater.*, *13*(14), 1069.
[14] Song, H., Park, B., Shin, K., Ohta, T., Takezoe, H. et al. *Adv. Mater.*, *16*(N 9–10).
[15] Song, H., Ha, N. Ya., Amemiya, K., Park, B., Takezoe, H. et al. (2006). *Adv. Mater.*, *18*, 193.
[16] Kogelnik, H. & Shank, C. V. (1972). *J. Appl. Phys. 43*, 2327.
[17] Yariv, A. & Nakamura, M. (1977). *J. Quantum Electronics*, *QE-13*, 233.
[18] Kopp, V. I., Zhang, Z.-Q., & Genack, A. Z. (2003). *Prog. Quant. Electron.*, *27*(6), 369
[19] Shabanov, A. V., Vetrov, S. Ya., & Karneev, A. Yu. (2004). *Pis'ma v Zhurnal Experimental'noi i Teoreticheskoi Fiziki*, *80*(#3), 206 (2004) (English translation: JETP Letters, *80*(#3), 181).
[20] Becchi, M., Ponti, S., Reyes, J. A., & OLdano, C. *Phys. Rev. E*, *70*, 033103.
[21] de Vries, H. (1951). *Acta Crystallogr.*, *4*, 219.
[22] Kats, E. I. (1971). *Sov. Phys.JETP 32*, 1004.
[23] de Gennes, P. G. & Prost, J. (1993). *The Physics of Liquid Crystals*, Clarendon Press: Oxford.
[24] Belyakov, V. A. & Dmitrienko, V. E. (1989). *Optics of Chiral Liquid Crystals, in Soviet Scientific reviews/Section A, Physics Reviews*, Khalatnikov, I. M. (Ed.), Harwood Academic Publisher: v. 13, 1–203.
[25] Belyakov, V. A. (1992). *Diffraction Optics of Complex Structured Periodic Media*, Springer Verlag, New York, Chapt. 4.
[26] Belyakov, V. A., Gevorgian, A. A., Eritsian, O. S., & Shipov, N. V. (1987). *Zhurn. Tekhn. Fiz.*, *57*, 1418 [*Sov. Phys. Technical Physics*, *32*(n7), 843–845 (English translation)]; *Sov. Phys. Crystalography*, *33* (n3), 337 (1988).
[27] Belyakov, V. A. (2006). *MCLC*, *453*(43), *Ferroelectrics*, *344*, 163 (2006).
[28] Matsushita, Y., Huang, Y., Zhou, Y., Wu, S. et al. (2007). *Appl. Phys. Lett.*, *90*, 091114.
[29] Moreira, M. F., Taheri, B., Palffy-Muhpray, P., & Belyakov, V. A. (2006). Book of Abstracts, 21st Int.Liq. Cryst. Conf., Kyestone, Colorado, USA, p. 405.